MDPI

Article

Nu—A Marine Life Monitoring and Exploration Submarine System

Ali A. M. R. Behiry *,† , Tarek Dafar †, Ahmed E. M. Hassan †, Faisal Hassan, Abdullah AlGohary and Mounib Khanafer

College of Engineering and Applied Sciences, American University of Kuwait, Salmiya 20002, Kuwait; s00051909@alumni.auk.edu.kw (T.D.); s00050792@alumni.auk.edu.kw (A.E.M.H.); s00051494@auk.edu.kw (F.H.); s00053561@alumni.auk.edu.kw (A.A.); mkhanafer@auk.edu.kw (M.K.)
* Correspondence: abehiry@auk.edu.kw
† These authors contributed equally to this work.

Abstract: Marine life exploration is constrained by factors such as limited scuba diving time, depth restrictions for divers, costly expeditions, safety risks to divers' health, and minimizing harm to marine ecosystems, where traditional diving often risks disturbing marine life. This paper introduces Nu (named after an ancient Egyptian deity), a 3D-printed Remotely Operated Underwater Vehicle (ROUV) designed in an attempt to address these challenges. Nu employs Long Range (LoRa), a low-power and long-range communication technology, enabling wireless operation via a manual controller. The vehicle features an onboard live-feed camera with a separate communication system that transmits video to an external real-time machine learning (ML) pipeline for fish species classification, reducing human error by taxonomists. It uses Brushless Direct Current (BLDC) motors for long-distance movement and water pump motors for precise navigation, minimizing disturbance, and reducing damage to surrounding species. Nu's functionality was evaluated in a controlled 2.5-m-deep body of water, focusing on connectivity, maneuverability, and fish identification accuracy. The fish detection algorithm achieved an average precision of 60% in identifying fish presence, while the classification model achieved 97% precision in assigning species labels, with unknown species flagged correctly. The testing of Nu in a controlled environment has met the system design expectations.

1. Introduction

The ocean covers 70% of Earth's surface, playing a critical role in sustaining and impacting life on Earth [1]. Despite this, humanity's knowledge of what species lie beneath its surface remains limited, as only 5% of oceans have been explored [2]. Exploring the ocean could provide us with the necessary knowledge for breakthroughs in medicine and vaccines or inspire advancements in bio-mimicry with the discovery of new marine species [3]. Such nature-inspired technologies have led to advancement in all fields, for example, reducing drag significantly in airplanes, or even cutting down costs on fuel consumption and emissions [4].

Although ocean exploration is crucial, exploring and studying marine life has proven to be a challenging endeavor over the years for researchers and scientists [5], for instance,

health risks to divers and limiting disturbance and damage to the ecosystem, as well as expeditions' costs. Firstly, exploration expeditions negatively affect marine life. The frequent physical contact between divers and the marine habitat has caused visible damage over the years [6]. The damage is partly caused by contact between the equipment of the divers and the organisms. In addition, increased coral skeletal porosity and decreased skeletal density due to ocean acidification have made coral reefs vulnerable to sustaining damage easily when in contact with divers or their equipment [7]. Although divers damaging marine life is mostly associated with mismanaged tourism and inexperienced divers, experienced divers also unintentionally cause damage, often with their fins.

The drawbacks and negative effects of ocean expeditions are not exclusively limited to marine life and organisms, as prolonged and frequent deep diving can cause serious health issues even to experienced divers. Divers frequently experience nervous system symptoms, commonly paraesthesia and concentration difficulties, after deep diving, and in some cases, the symptoms include seizures and temporary memory loss [8]. The negative effects are not limited to the nervous system. Diving in general risks health complications, as it puts the cardiovascular system, ears, and lungs under substantial stress, while in some cases it increases the chances of decompression sickness [8].

Aside from the negative effects on both marine life and divers, ocean exploration expeditions can be costly and time-consuming. The costs can be broken down but are not limited to equipment costs, ship renting/buying, hiring/training divers, as well as having a marine specialist present on board to identify any previous or new fish species in real time. One of the aims of the proposed ROUV is to reduce human error while identifying fish species; however, having a marine specialist on board is crucial in order to validate the data displayed during a mission.

To tackle these issues, Remotely Operated Vehicles (ROVs) or Remotely Operated Underwater Vehicles (ROUVs) are introduced. ROUVs reduce the number of professionals needed on board to carry out expeditions and avoid the health risks discussed earlier that are imposed on divers. ROUVs, however, have a limited depth of exploration due to their tether. Continuously, the tether is at risk of getting tangled with itself or with debris during operation. In some cases, an ROUV operates autonomously or wirelessly, eliminating the need for an operator or a tether [9]. However, having an Autonomous Underwater Vehicle (AUV) introduces more issues, such as the AUV never returning from operation, being stuck and unable to free itself, and taking away the privilege of exploring freely since AUVs operate based on a predetermined path or input from the environment [10,11].

One of the challenges of designing a wireless ROUV is the rapid attenuation of high radio frequency underwater [12]. In this paper, we introduce a solution that utilizes low radio frequency, specifically Long Range (LoRa) [13–16]. LoRa prevails in underwater communication when compared with other high-frequency technologies like Wi-Fi and Bluetooth due to the nature of signal attenuation underwater. The relationship between signal attenuation and frequency is proportional, meaning that the higher the frequency the higher the signal attenuation. In addition to operating at low frequencies, LoRa minimizes its power consumption significantly when compared with other communication technologies [17]. Having a tetherless connection means that the ROUV has a limited power supply, making the low power consumption a beneficial feature for longer missions.

The ROUV proposed in this paper utilizes machine learning (ML) to identify fish species, offering a low-cost, scalable alternative to traditional diving. In addition, it minimizes human error, enhances data collection on migration patterns and fish habitat, is accessible for education, and promotes marine life conservation efforts.

Given the aforementioned information, in this paper, we introduce Nu (a name inspired by an ancient Egyptian deity representing the primordial waters), a machine learning

leveraged ROUV system designed for marine life monitoring and exploration, with the following key contributions:

- Designing and implementing a Remotely Operated Underwater Vehicle (ROUV) from scratch, utilizing 3D modeling and printing. The use of mainly biodegradable materials for 3D printing ensures both cost efficiency and environmental sustainability in the final product. Therefore, most of the external body of the ROUV may be 3D printed on demand, providing further replicability.
- Utilizing LoRa as the main communication technology between the operator and ROUV, allowing for real-time long-range usage and power efficiency; a novel contribution according to our research.
- Implementing an ML model at a base station that wirelessly receives the live-feed video from the onboard camera to both identify fish and classify said fish into multiple species classes. Furthermore, the model is capable of flagging unknown fish species for the discovery of new species.
- Conceptualizing and implementing two modes of operation: a propeller-based mode and a water-pump-based mode. The propeller-based mode would allow the ROUV to travel to the desired mission's location quickly, while the water-pump-based mode would allow the ROUV to navigate close to marine life without causing any major disturbance or harm.
- Combining the aforementioned contributions into a functional prototype that is deployed and tested in water and shown to be ready for marine life exploration.

The remainder of this paper is structured as follows: Section 2 reviews related literature on previous work regarding other ROVs, AUVs, and ML models. Section 3 details the system's design and methodology, including communication, locomotion, and ML pipeline design. Section 4 presents the implementation, covering waterproofing, circuitry, and full assembly. Section 5 discusses experimental results, including waterproofing, underwater communication, motor functionality, and ML model performance. Finally, Section 6 concludes this paper, highlighting the system's contributions and potential impact on marine exploration.

2. Literature Review

This section discusses and provides an overview of existing relevant work on ROVs/ROUVs, AUVs, and a combination of both. In addition, this section also covers work in the literature related to Artificial Intelligence (AI) models capable of fish species detection and classification.

The authors in [18] implemented a wireless ROV with an educational goal. The ROV's design is inspired by the Seawolf submarines. The authors opted to use a wooden mold that was later on cast with fiberglass. The ROV operates using a single Brushless Direct Current (BLDC) propeller motor allowing forward and reverse movement. In addition, it utilizes fins to navigate through the water, with the help of servo motors. The ROV was designed to be controlled wirelessly using a remote controller and a 2.4 GHz receiver. The ROV was tested for a maximum transmission range of 180 m above the water's surface. The ROV utilized lead acid and lithium polymer (Li-Po) batteries to power the motors and the water pump respectively, achieving 1 h operating time [18].

In [19], an AUV is proposed that is able to "dynamically change" the structure of the body and positions of the motors, allowing the AUV to explore and navigate through tight spaces such as shipwrecks and underwater cave systems. The AUV can receive commands wirelessly from a laptop, The AUV follows a predetermined path that is planned before the mission, and the operator needs to send instructions of the specific yaw, pitch, etc., angles,

as well as the desired depth. Using onboard sensors, the AUV then compares the desired angle with the actual angle and adjusts the positions and thrusters' power accordingly [19].

Another AUV proposed by [10] aimed to inspect and monitor the growth of seaweed farms autonomously. Mission planning is conducted on a software system called Neptus where the operator is able to stop, pause, replace, or resume a running mission plan. The AUV localizes the farm relative to its position and then determines the rough outer lines of the farm. The mission is then started and the AUV begins heading to the specified location using a GPS module onboard. Once the AUV arrives at the location, it begins scanning the seaweed using a 2D sonar. Aside from the 2D sonar, the AUV utilizes acoustic technology for any underwater communication needed between itself and the operator. The authors did not utilize a camera since water visibility around farms is low, which would hinder the AUV's scanning ability. Once the AUV has successfully followed the specified path, it heads back to base. The AUV uses counter-rotating propellers allowing forward and backward movement and implements a thrust vectoring nozzle for maneuvering [10].

The authors in [20] propose an ROV that is capable of six degrees of freedom, identifying benthic species, following desired routes, detecting cracks, and analyzing obstacles. The ROV has a battery life of 3 h and is tethered. The mentioned ROV can reach up to 7 m underwater, however, it is not mentioned whether this is due to the length of the tether used or the ROV's pressure-handling capabilities. The benthic species recognition is based on geometric shapes; however, the dataset did not include images of specific benthic species. Moreover, the ROV is capable of following specifically red lines at the bottom of a pool and avoiding obstacles that were represented as cubes placed on the pool's floor. Crack detection was tested successfully and showed positive results [20].

In [21], Aguirre-Castro et al. developed and implemented a tethered ROV that can reach up to 100 m underwater while having a battery life of 2 to 3 h. Testing was conducted on monitoring cracks in polyvinyl chloride (PVC) pipes located at the seabed, which the ROV performed successfully. The ROV is equipped with a camera which is installed at the lower part of the ROV to carry out the pipe inspection. The ROV is controlled using a Graphical User Interface (GUI) on a computer. The body of the ROV was made out of PVC pipes, which were filled with steel rods in order to reach the desired weight and buoyancy [21].

The authors in [22] designed the SPARUS II ROUV for versatility. It is a lightweight underwater vehicle with hovering and long-range capabilities, supported by a robust propulsion system. The primary goals in designing SPARUS II were to create a cost-effective, maneuverable, and easily deployable AUV. SPARUS II offers two modes of transportation: hovering mode and torpedo-based mode. When operating in the hovering mode, its estimated maximum velocity in surges is between 3 and 4 knots, with 3 thrusters for controlling the surges, heave, and yaw. In torpedo-based mode, two fins are installed behind the two horizontal thrusters to control the depth and maintain a stable angular position in roll. It is able to reach a maximum depth of 200 m and can remain operational from 8 to 10 h [22].

The submarine discussed in [23] aims to use Near-Infrared (NIR) Spectroscopy to detect and collect microplastics in the ocean. The design consists of three main sections, an outer hull, an inner hull, and a pressure hull in between the two that decides the maximum depth the submarine can dive. The micro-objects pass through a pipe with a filter paper to separate the water, then a motor pushes the objects through onto a conveyor belt that moves them under a spectrometer to determine whether they are microplastics or not. This approach aims to reduce the inefficiencies and environmental harm associated with traditional detection methods. At the same time, the authors underline the need

for further refinement of the detection algorithm and integration of ML for improved accuracy [23].

In [24], a submarine was developed using a 30 cm PVC pipe and metal sheets. PVC was used due to its ease of fabrication, comparatively low cost, low weight, reliability and sustainability, recyclability, and a high degree of inertness and resistance to corrosion, while the metal sheets were used to fit the motors. A container was fitted inside the hull to be filled with water to match the submarine's density with the water outside. For effective displacement, propellers were fitted to 4 DC geared motors which were powered by two lead acid batteries, and the whole body was waterproofed using a glue gun and epoxy resin. The submarine used multiple 35 m wires taped together to communicate with the surface [24].

The work in [25] proposed the deployment of low-data-rate acoustically controlled ROVs. In [25], the Blue Robotics BlueROV2 was used as the remotely operated submersible platform. Two Arduino MKR WAN 1300 microprocessors/radios, which offer LoRa radio frequency connectivity, along with MAVlink messages were used to develop half duplex tether-free communication between the Ground Control Station (GCS) and the ROV. The LoRa radios connect the GCS's MAVProxy to the ROV's Proxy, which is run on a Raspberry Pi. The Raspberry Pi, in turn, acts as an intermediary between the GCS and the Pixhawk. The Pixhawk acts as a real-time controller to maintain altitude and control the motors. The system was tested in both large and small water tanks and the successfully transmitted and received packets were measured. At a distance of 3 ft, while the ROV was on the surface, all packets were successfully transmitted and received, while 60% were successful underwater. The submarine was responsive after informal testing in a 3 ft pool. The system uses an instruction-based system, where the ROV awaits instructions from the operator and stops receiving new ones until the last instruction is done [25].

The authors in [26] develop an ROUV that tackles the detection and collection of underwater plastic waste through a ML model installed on a Raspberry Pi. For the body of the ROUV, PVC pipes were chosen as the material for the body frame, and both a float and a camera were installed on the top and bottom of the frame respectively, while a propeller was attached to help the body move. The Raspberry Pi was used to control all primary functions, including image processing, motor control signal transmission, managing the ROUV position, and capturing plastic waste. The YOLOv3 model was also installed on the Raspberry Pi. The estimated current consumption for one hour was 3000 mAh, and the maximum depth was 10 m. After testing, it was determined that the effective threshold for object detection is around 100 NTU, with an average confidence score of 77%.

The study in [27] proposed a method for the inspection of hull surfaces with the use of Convolutional Neural Networks (CNNs) equipped on an ROUV. The tethered ROUV used was developed by SLM Global to clean underwater hull surfaces. It attaches itself to the hull surface and crawls along it using electrically driven magnetic wheels. Two brushes installed on the bottom are used to clean the surface of the hulls. The classification was carried out using a soft voting ensemble of the well-known CNN models DenseNets, EfficientNets, Inceptions, MobileNets, ResNets, and VGGs. The optimal weights of each were selected using transfer learning. The classification accuracy and F1-score were approximately 98.13% and 98.11%, respectively.

Furthermore, there have been several works in the literature that targeted fish identification and classification problems. In [28], a novel Transformer-based method for fish image classification was proposed. The method introduced claims an efficient handle of images of different resolutions and excellent generalization ability. It is capable of distinguishing between low-resolution marine fish images and high-resolution freshwater fish images. Furthermore, a label smoothing loss function was introduced to alleviate over-fitting and

overconfidence issues, and data augmentation techniques such as cropping and random flipping were used to enhance the model's robustness. Finally, pre-trained model weights were implemented to expedite the training process [28].

In [29], as an alternative to standard tracking technology, a fish passage observation platform to monitor fish was developed. An automated real-time deep learning framework was included in order to analyze the data. First, a YOLO model was included to accurately detect and classify eight species of fish. Following this, a Norfair object tracking framework was added to track and count the fish [29].

According to the works in the aforementioned literature, there is a lack of work on a complete ROUV system for the fish classification problem. Additionally, there is a notable research gap when it comes to recent ROUV technology, as most studies focus on AUVs. Moreover, not many works make use of different communication technologies such as LoRa to tackle the underwater communication range issue. The use of a LoRa module for underwater wireless communication between the remote control and the submarine body presents a novel approach to achieving tether-free control. While previous works such as [25] have explored this technology, they have not addressed additional features that Nu incorporates, such as real-time control, cost efficiency, power efficiency, and environmentally friendly design as well as the use of ML for fish identification and classification based on external features. Although ML has been applied in some underwater applications, and fish detection and classification have been previously explored in some reviewed works such as [28,29], none of the reviewed works have integrated an ML model for these tasks within the ROUV itself based on our research. The approach in Nu not only detects and classifies the fish species in the dataset but also fills a gap by allowing the model to identify anomalous species not introduced in the training data. This increases the real-world applicability of the system, making it more robust for marine life monitoring and exploration. Table 1 demonstrates a comparative study between all of the discussed works throughout Section 2 and the proposed ROUV system.

Table 1. Comparative study of referenced works relevant to the proposed ROUV.

Reference	Propulsion Method	Communication Method	Special Features
[18]	BLDC motor with fins	2.4 GHz wireless	Designed for education; max range of 180 m above water
[19]	Dynamic motor positioning	Wireless commands from a laptop	Navigates tight spaces such as caves and shipwrecks
[10]	Counter-rotating propellers	Acoustic communication	Inspects seaweed farms; uses 2D sonar for scanning
[20]	BLDC motors	Tethered	Identifies benthic species; follows routes and detects cracks
[21]	PVC pipe-based thrusters	Tethered	Inspects PVC pipes at seabed; operational depth of 100 m
[22]	Thrusters and fins	WiFi, Xbee, GSM/3G, acoustic modem	AUV; lightweight design; operational depth of 200 m
[23]	Motor-driven conveyor belt	Not specified	Uses NIR spectroscopy for detecting microplastics
[24]	DC geared motors with propellers	Tethered	Cost-effective; waterproofed using epoxy and glue gun

Table 1. *Cont.*

Reference	Propulsion Method	Communication Method	Special Features
[25]	BlueROV2 platform	LoRa (433 MHz)	LoRa-based tether-free communication with MAVLink integration
[26]	Propeller-based motion	Tethered	Detects and collects plastic waste using YOLOv3
[27]	Electrically driven magnetic wheels	Tethered	Cleans hull surfaces; uses CNN for defect detection
Nu	BLDC and Water pump motors	LoRa (433 Mhz)	Utilizes an ML pipeline to detect and classify fish species; Minimizes disturbance and damage to marine life.

3. Methodology and Design

This section illustrates the proposed system model and the 3D design process of the ROUV body.

3.1. System Model

Before implementing the ROUV, the system model illustrated in Figure 1 was created to outline the fundamental components necessary for its operation. The diagram highlights the communication mediums utilized between the operator and the ROUV, as well as between the ROUV and the ML model. As observed in Figure 1, the operator controls the ROUV using a wireless controller. Moreover, the live video feed is also transmitted wirelessly from the onboard camera to the laptop, where it is fed to the ML model. The ML model then identifies, classifies, and records any instances of fish found in real-time, allowing the operator the freedom to explore unhindered.
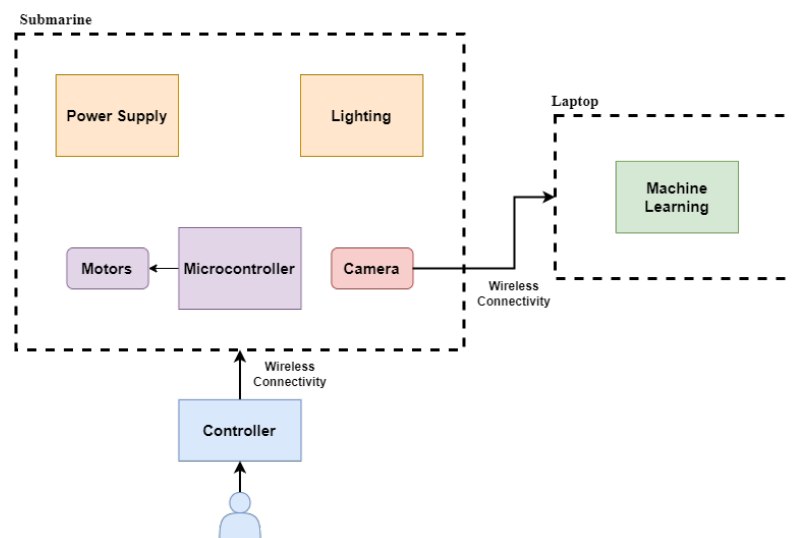

Figure 1. ROUV system model.

3.2. Locomotion

As previously mentioned in Section 1, divers can cause harm and disturbance to the surrounding habitat or marine life. However, this can also be the case in ROUVs if propeller-based movement systems are utilized, if the ROUV is no longer motile, or its guidance system is flawed. As such, the proposed ROUV in this paper utilizes two modes

of locomotion. When the ROUV is first deployed, it utilizes propeller-based motors, specifically BLDC motors, to travel to the specified exploration area. This mode will be mainly used near the surface of the water, away from any fish or habitat. Once the ROUV reaches its destination, the operator switches to the precision mode. In this mode, the operator is able to utilize the surrounding water in propelling the ROUV with the help of water pump motors. These motors are significantly weaker and quieter than the BLDC motors but have enough torque to push the ROUV, making them an ideal fit for the application. This eliminates any disturbance and harm that could be caused due to the propellers spinning at high speeds.

3.3. Exterior Design

The body of the ROUV is 3D printed using carbon fiber polylactic acid (PLA) on a Fused Deposition Modeling (FDM) 3D printer. To ease the printing process and simplify assembly and disassembly, the ROUV's body is constituted by the parts shown in Figure 2 which were designed using SolidWorks. Moreover, the ROUV is designed to be symmetrical for stability underwater. The exact dimensions (length × width × height) in millimeters for each part are as follows:

- Figure 2a: 140 × 170 × 200.13 mm.
- Figure 2b: 130 × 93.87 × 93.87 mm.
- Figure 2c: radius of 50.2 and 25.41 mm thick.
- Figure 2d: 167 × 20 × 30 mm.
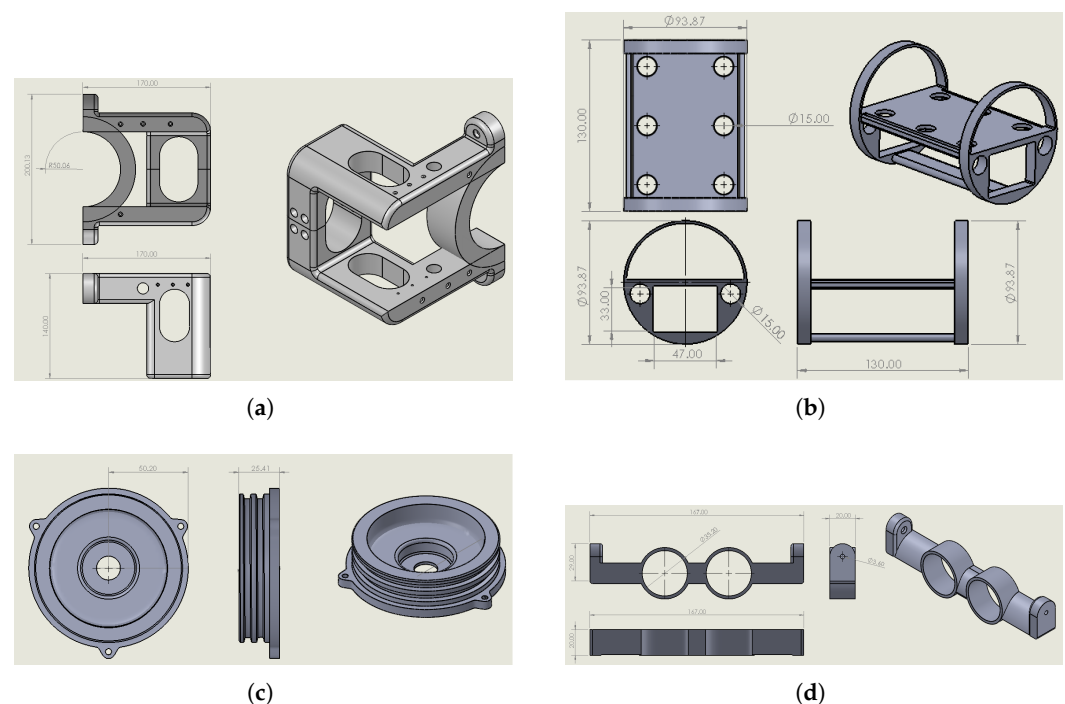

(**a**)

(**b**)

(**c**)

(**d**)

Figure 2. Three-dimensional-designed parts of the ROUV's body: (**a**) Exterior body piece used to hold the WTC. (**b**) Component holder to house the components inside the WTC. (**c**) End-cap design to seal the WTC. (**d**) Syringe holder design.

The body of the ROUV consists of four symmetrical 3D-printed pieces at each corner. The piece is shown in Figure 2a. Any unused surfaces of the piece are hollowed out in order to reduce the material cost while printing, and to minimize water drag. The pieces have a curved edge equal to the diameter of the Water Tight Chamber (WTC). The WTC is an acrylic tube that is water-sealed from both ends using 3D-printed end-caps in Figure 2c. The end caps are equipped with O-ring grooves that allow wires to pass through to the

motors. This acrylic tube houses all the electrical components and is transparent. In case the pressure inside the WTC becomes an issue in the testing phase, the end caps are designed with three mounting points for threaded rods. These rods would pass through both end-caps, preventing them from popping out, making the design suitable for deeper diving. In addition, the end-caps are hollowed from the middle in order to pass a wire gland. This wire gland would be tightened on the wires passing to the outside, preventing water leakage to the WTC.

In order to control the buoyancy of the ROUV, a system consisting of two syringes and a tubing system with peristaltic motors is implemented. The syringes are used to hold 200 mL of air in total to decrease or increase the buoyancy accordingly. To hold these syringes in place, a syringe holder is designed as shown in Figure 2d. The syringe holder is screwed to the exterior body piece shown in Figure 2a. The syringes are inserted and secured into the two O-openings of the syringe holder.

Finally, as previously mentioned, the center of mass is important to maintain underwater stability. As such, a component holder was designed to prevent the components from moving freely in the WTC, thus maintaining the center of mass, securing the components in place, and allowing for fluid and secure motion in the water. The component holder design is shown in Figure 2b.

The component holder is designed to hold a $20 \times 5 \times 5$ cm, 11.1 V 6000 mAh Li-Po battery, an Arduino UNO microcontroller, a camera, and several electrical components (like relays). Moreover, the holder has circular openings to allow the wires to pass from one end to the other in any direction.

A simulation of the ROUV fully assembled using these parts was conducted as illustrated in Figure 3. In this figure, we show how all the parts in Figure 2 give the final shape of the ROUV. Apparent in this figure is how the WTC will house the complete electrical components on the component holder.
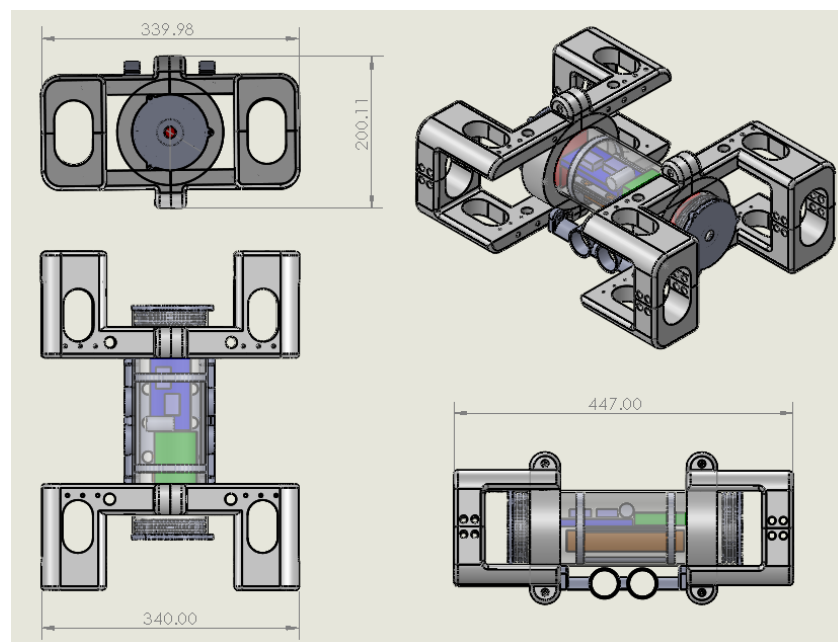

Figure 3. Full 3D design assembly simulation.

3.4. Maximum Depth Analysis

The maximum depth that the ROUV can safely operate is determined by the water pressure at depth and the structural integrity of the Water Tight Chamber (WTC), primarily

made of acrylic. The pressure at a given depth, h, is calculated using the hydrostatic pressure formula [30]:

$$P_{\text{total}} = P_{\text{surface}} + \rho g h, \tag{1}$$

where P_{surface} is the atmospheric pressure at the surface (approximately 101,325 Pa or 1 atm), ρ is the density of water (1025 kg/m^3 for seawater), g is the acceleration due to gravity (9.81 m/s^2), and h is the depth in meters.

The critical pressure that the structure can withstand before failure is estimated using the thin-walled cylinder formula for buckling [30]:

$$P_{\text{critical}} = \frac{2E}{(1 - \nu^2)} \left(\frac{t}{D} \right)^3, \tag{2}$$

where E is the Young's modulus of acrylic (3.2×10^9 Pa), ν is the Poisson's ratio for acrylic (approximately 0.35), t is the wall thickness of the acrylic tube, and D is the outer diameter of the tube. Given $t = 5$ mm and $D = 100$ mm, the critical pressure is approximately $P_{\text{critical}} \approx 912{,}000$ Pa (9.01 atm). The maximum depth, h_{max}, is calculated by equating the hydrostatic pressure to the critical pressure [30]:

$$h_{\text{max}} = \frac{P_{\text{critical}} - P_{\text{surface}}}{\rho g}, \tag{3}$$

substituting the values gives $h_{\text{max}} \approx 80.6$ m. Thus, the ROUV is estimated to safely operate up to a depth of approximately 80.6 meters under seawater conditions. To account for material imperfections and unforeseen stresses, a safety factor of 1.5 is applied, limiting the operational depth to approximately $h_{\text{safe}} \approx 53.7$ m [30].

3.5. Machine Learning Pipeline

This section gives an overview of the final implementation of the ML pipeline. Details regarding each step in the model's development process will be explained more thoroughly in Section 4.4.

As previously stated, Nu allows detecting and classifying different fish species by implementing different ML models. A camera, with a resolution of 720p at 60 frames per second, installed on the submarine captures live-feed footage and sends it to a base station above water. Each frame captured by the camera is first passed to a YOLOv8 object detector [31]. The detected fish in each image are cropped individually. Following this, these cropped images are resized to 224×224, as it is the expected input size for the next stage in the pipeline. Captured images are then passed to a ResNet50 classifier before a threshold of 50% is applied [32]. This threshold acts as a filter so that any detected fish with a confidence score below the threshold is discarded. Otherwise, the cropped image is classified into one of two categories: known and unknown. The dataset could be expanded to include any number of fish classes. However, the creation of an inclusive dataset representative of the thousands of known fish species is outside the scope of this project. Therefore, the known fish species included were Blacktip (*Carcharhinus limbatus*), Clownfish (*Amphiprion ocellaris*), Eagle ray (*Aetomylaeus bovinus*), Emperor Angelfish (*Pomacanthus imperator*), and Jellyfish (*Cassiopea andromeda* and *Catostylus perezi*). The unknown category is reserved for anomalous data points outside the five known species, or in other words, species that were not present in the dataset while training. A pseudocode of the ML pipeline is provided in Algorithm 1.

Algorithm 1 Machine Learning Pipeline.

1: **procedure** FISH CLASSIFICATION PIPELINE
2:     Load *YOLO Model* ← Model File Path
3:     Load *ResNet Model* ← Model File Path
4:     *classNames* ← *Blacktip, Clownfish, Eagle ray, Emperor Angelfish, Jellyfish, Unknown*
5:
6:     def *crop fish from frame* (frame, boundingBox):
7:     cropped fish ← frame[boundingBox]
       return cropped fish
8:
9:     def *Classify fish species* (ResNet, cropped fish):
10:     *img* ← resize cropped fish to (224,224).
11:     *img* ← Convert cropped fish to required format for classification.
12:     *img* ← Add batch dimension to prepare for model input.
13:     *img* ← Preprocess img.
14:     *predictions* ← Pass img to ResNet model.
       return predictions
15:     *cap* ← video capture from camera.
16:     *threshold* ← 0.5.
17:     **while** True **do**
18:        *ret, frame* ← read frame.
19:        **if** not ret **then**: **break;**
20:        *results* ← Pass frame to YOLO model.
21:        **for** result in results.boxes.data.tolist() **do**
22:            $x1, y1, x2, y2, conf, classid$ ← *result*.
23:            **if** conf > threshold **then**
24:               draw bounding box.
25:               *cropped fish* ← crop fish from frame.
26:               *predictions* ← classify fish species method.
27:               $img ← resize(cropped fish, (224, 224))$.
28:               *classID* ← index of max prediction.
29:               *confidence* ← value of max prediction.
30:               *className* ← classNames[classID].
31:            **if** confidence > 0.80 **then**:
32:               Display class name.
33:            **else**
34:               Display Unknown.

The machine learning pipeline in Algorithm 1 begins by loading the pre-trained YOLO model for object detection and the ResNet model for fish species classification, along with defining a list of target class names, including the aforementioned specific fish species and an "Unknown" category. A helper function is defined to crop fish from the video frame based on bounding box coordinates from the fish identification model, and another function prepares the cropped image for classification by resizing, converting it into a suitable data format, and preprocessing it for input into the ResNet model. The pipeline captures video frames in real time and passes each frame to the YOLO model to detect fish, returning bounding boxes and confidence scores for the detections. For each detection exceeding a specified confidence score threshold, the bounding box is drawn, and the cropped fish image is classified using the ResNet model. The classification process identifies the fish species with the highest confidence score, and if this score exceeds 80%, the species name is displayed; otherwise, the output is set to "Unknown". The loop continues until the video feed ends, enabling the system to perform continuous fish detection and classification.

4. Implementation

This section details the implementation of the proposed ROUV including circuitry, assembly, and the ML model for fish species classification.

4.1. Waterproofing

Waterproofing plays a crucial part in the implementation, as it prevents damage to the electronics and avoids serious hazards such as explosions and toxic fumes when in contact with the Li-Po battery. Moreover, as previously mentioned in Section 3, all of the 3D designs discussed in Section 3 were 3D printed using carbon fiber PLA on an FDM 3D printer. It is crucial for the WTC to be sealed such that it does not allow water through.

To a certain extent, all 3D printing materials are hygroscopic by nature, that is, they absorb water [33]. As observed in Figure 4, while the layers are being printed on an FDM 3D printer, microscopic voids are produced. Under normal circumstances, these microscopic voids are insignificant, however, these voids become an obstacle when the 3D part is submerged underwater for a prolonged period of time, especially when placed under pressure as the depth increases. The voids do not pose any threat to the electrical components since the body is separated from the WTC, but since the prints are printed at a 35% infill, these voids allow water to seep through and settle in the air pockets inside the 3D prints, ultimately increasing the weight, which in turn decreases buoyancy. Greater depths could lead to the end-caps popping out and flooding the WTC, or the ROUV sinks and is lost. To overcome this, two layers of epoxy resin, composed of Bisphenol-A Diglycidyl Ether (DGEBA) as the base resin and a cycloaliphatic amine curing agent, were applied to the 3D prints. This composition allows the epoxy to seep into the voids and cure, forming a cross-linked thermoset structure that effectively blocks any water from seeping in [34]. After waterproofing each 3D print, the WTC was assembled using the end caps, O-rings, and waterproofing wire glands.
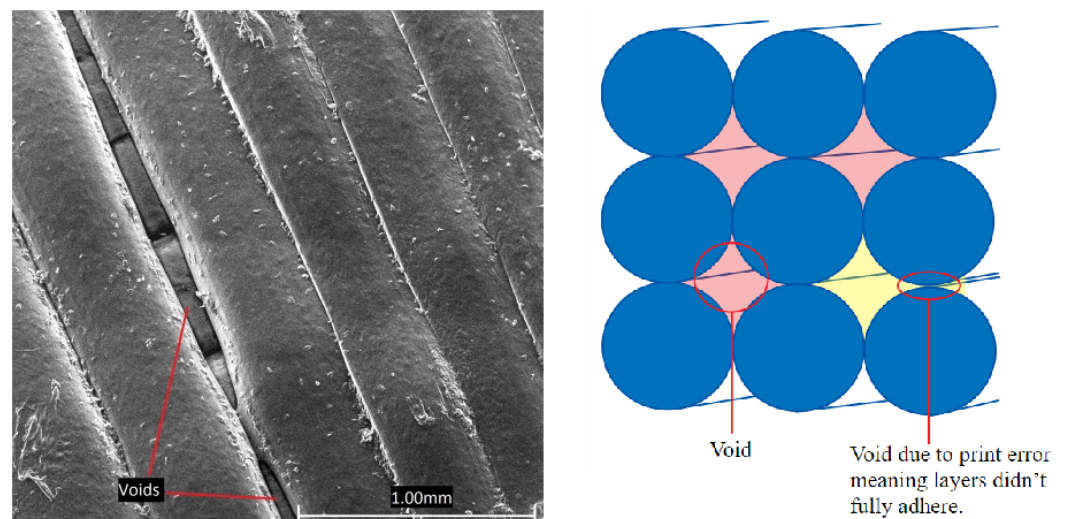

Figure 4. Printing structure of FDM printers [35].

4.2. Circuit Implementation

This subsection overviews the implementation of both the transmitting and receiving circuits of the ROUV.

4.2.1. Transmitting Circuit

LoRa is a low-power-consumption, low-frequency radio technology capable of reaching up to 3 km in a suburban area with dense residential dwellings [13] and up to 7 m underwater [36]. Continuously, it is the main communication technology between the

operator and the ROUV. The transmitting circuit consists of an Arduino UNO R3 [37] connected to a LoRa SX1278 module [38]. LoRa operates between 169 MHz and 915 MHz depending on the region. In this case, the frequency used is 433 MHz. In addition to the microcontroller and LoRa module, two joysticks are utilized [39]. These components together make up a controller for the ROUV.

As observed in Figure 5, the controller circuit consists of an Arduino UNO, a LoRa module, three pull-up resistor buttons, and two joysticks. The two joysticks will be used to control the 12 V bi-directional BLDC motors as well as four 12 V water pump motors. Next, the first button is used to switch between control modes, the long-distance mode consisting of the BLDC motors, and the quiet/precision mode consisting of the water pump motors. While in precision mode, the other two buttons are used to control two 12 V peristaltic pump motors connected to the syringes. These peristaltic pumps are used for sinking and surfacing the ROUV by pumping water in and out of the 100 mL syringes, ultimately increasing and decreasing the weight of the ROUV by 200 g in total.
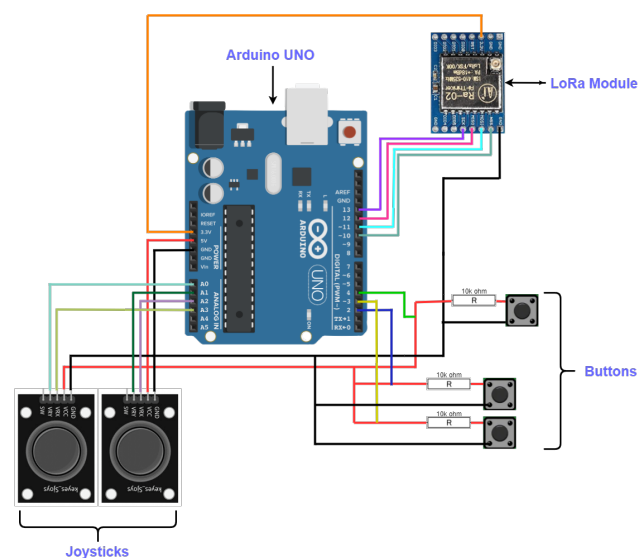

Figure 5. Controller circuit diagram.

4.2.2. Receiving Circuit

Similar to the transmitting circuit, the receiving circuit also consists of an Arduino UNO and a LoRa module to communicate with the controller as observed in Figure 6. Alongside the microcontroller and the LoRa module, the circuit consists of two 4-Channel relay modules [40] that control four water pump motors and two peristaltic pump motors, as well as two Electronic Speed Controllers (ESCs) that are connected to the BLDC motors. In addition to these components, the circuit also consists of an infrared-controlled 1-Channel relay module, a fuse, and the 11.1 V 6000 mAh Li-Po battery mentioned earlier. As mentioned in Section 3.3, the acrylic tube is completely transparent, which allows the utilization of an infrared-controlled relay. This relay is used to remotely connect and disconnect the battery from the rest of the circuit, which maximizes the battery life and eases the process of powering on the ROUV without removing the end-caps. As an additional safety measure, a 2 A fuse was connected in series with the battery, which would break in case of a short circuit while the ROUV is operational underwater. Since the operational voltage of all the components is 12 V, it should be noted that the components are connected in parallel with one another.
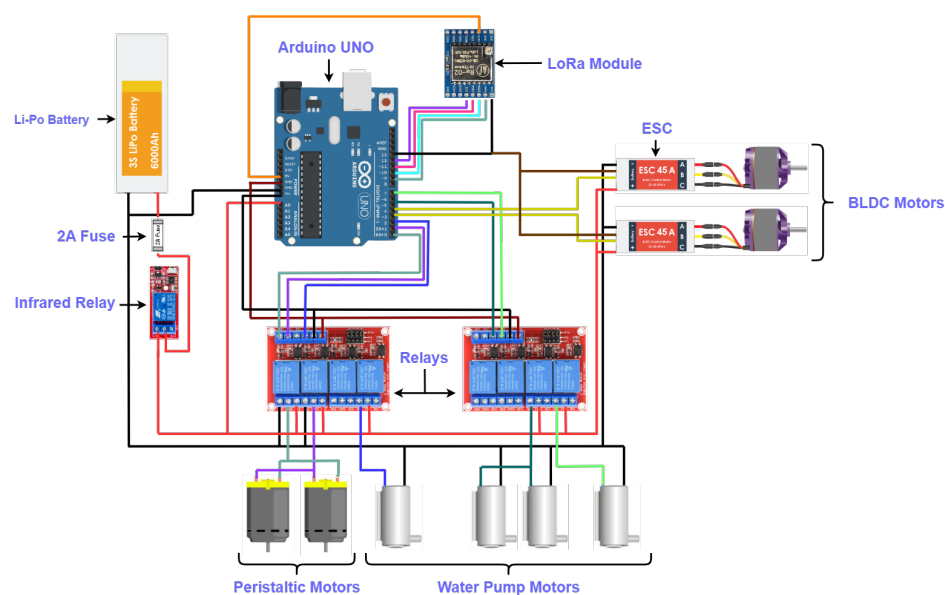
Figure 6. ROUV circuit.

In addition to these components, a compact bullet camera is also utilized. However, the LoRa module used, or any low radio frequency technology, is incapable of transmitting a live video feed due to the low bit rate. To overcome this limitation, a separate communication system is required. The system consists of a 2.4 GHz transmitter and receiver modules directly connected to the camera. As previously discussed in Seciton 1, high radio frequency attenuates easily as the signals penetrate the water. As such, Figure 7 showcases the camera system which consists of an air-tight container floating above the water's surface, housing the transmitter connected to the camera and a separate 9.8 × 5.9 × 2.1 cm 11.1 V, 4000 mAh Li-Po battery for the transmitter and camera. The technical specifications of the components mentioned throughout this section are listed in Table 2.
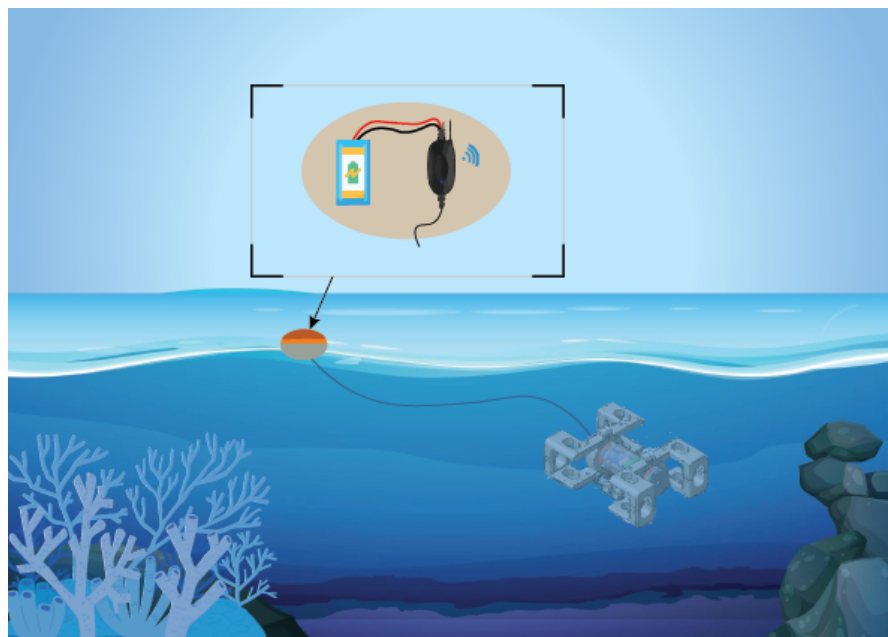

Figure 7. ROUV camera system.

Table 2. Technical specifications of components used in the ROUV.

Component	Specifications
LoRa SX1278 RA-02	• Frequency: 433 MHz. • Operating Voltage: 1.8–3.7 V. • Output Power: 100 mW. • Sensitivity: −148 dBm. • Range: Up to 7 m underwater [36].
Arduino UNO R3	• Microcontroller: ATmega328P. • Operating Voltage: 5 V. • Digital I/O Pins: 14 (6 PWM outputs). • Analog Input Pins: 6. • Power Supply: 7–12 V.
Water Pump Motor	• Operating Voltage: 12 V. • Power Consumption: Approximately 10 W. • Current Draw: Approximately 0.83 A. • Submersible: Yes.
BLDC Motor	• Operating Voltage: 12–16 V. • Power Consumption: Up to 200 W. • Current Draw: Approximately 12.5 A. • ESC: bi-directional 45 A. • Submersible: Yes.
Peristaltic Pump Motor	• Operating Voltage: 12 V. • Power Consumption: Approximately 3.6 W. • Current Draw: Approximately 300 mA. • Submersible: Yes.
Bullet Camera	• Operating Voltage: 12 V. • Power Consumption: Approximately 1.8 W. • Current Draw: Approximately 0.15 A. • Minimum Illumination: 0.01 Lux, suitable for low-light conditions. • FOV: 120° at 720p HD.
ROUV Li-Po Battery	• Voltage: 11.1 V. • Capacity: 6000 mAh. • Charge Time: Approximately 2 h.
Camera System Li-Po Battery	• Voltage: 11.1 V. • Capacity: 4000 mAh. • Charge Time: Approximately 1 h.
Syringes	• Capacity: 100 mL each (2 used).

4.3. Full Assembly

Using the circuit designs discussed in Section 4.2 and the component holder in Figure 2b, the ROUV electronics were implemented and placed inside the WTC, and the controller circuit was implemented.

The BLDC motors, peristaltic pump motors, and the syringe holders were screwed to the printed pieces shown in Figure 2a, and the wires were passed through the glands to the

motors. The WTC was then placed between the four pieces which were tightened together. Figure 8 demonstrates an annotated top view of the assembled ROUV. Each annotation, 1 to 7, is as follows:

1. BLDC motors that are used for long-distance travel. These motors can rotate clockwise and anti-clockwise, allowing the ROUV to move forward and backward, as well as turn left and right.
2. Water pump motors at the back of the ROUV that are used for precise forward movement.
3. Water pump motors on each side that are used for precise left and right turns.
4. Peristaltic motors that allow the syringes to be filled with water for sinking and surfacing.
5. Syringes.
6. Scuba diving flashlights used to illuminate in front of the ROUV.
7. WTC that houses all of the circuitry and electronics.

It should be noted that each flashlight has its own battery that can last up to 8 h. This is beneficial since connecting LEDs to the battery inside the WTC would reduce the battery life significantly; moreover, having a separate power source for lighting simplifies the circuit and reduces overall cost. Finally, Figure 9 demonstrates the ROUV while operating underwater during testing. As observed, the ROUV is fully operational using LoRa without any tether, excluding the wires of the live-feed transmitting system that was mentioned previously.
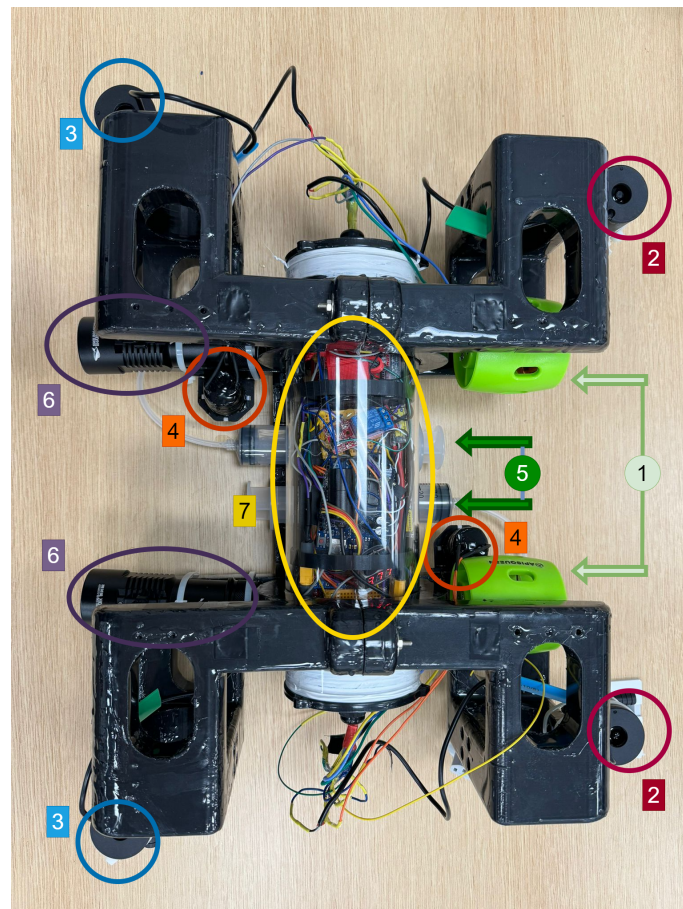

Figure 8. ROUV assembled.

Figure 9. ROUV operating underwater.

4.4. Machine Learning Model

Underwater fish identification and classification are met by many challenges, such as complex image backgrounds, poor visibility, and biological variability in fish appearance. As such, we develop a ML pipeline that allows the real-time detection and classification of fish species. The pipeline also aims for the identification and flagging of any anomalous data points. This allows the model to recognize new species that were not present in the dataset during training. To that end, both object detection and object classification models were implemented, along with popular techniques such as anomaly detection, transfer learning, and data augmentation.

The ML pipeline processes a real-time video feed captured by the camera installed on the submarine body. The camera, with a resolution of 720p at 60 frames per second, transmits the video feed wirelessly to a laptop above water. Frames are sampled continuously to ensure real-time processing without latency. Each sampled frame captured from the live feed is fed to the object detection model. In this case, the YOLOv8 algorithm was used to train the object detection layer [31]. The object detector's task is to detect the location of the fish in each frame. A threshold of 50% is first applied. The model attempts to identify fish in the image, if the object is identified as a fish with a confidence score over 50%, then it is flagged as a fish and its coordinates are output. A bounding box is drawn around each detected fish using the output coordinates of the model. The fish in the frame are then cropped into separate images and each cropped image is resized to 224×224 before being passed to the classifier. The cropping step significantly reduces the impact of complex underwater backgrounds, which often hinder fish classification. The model was trained on a dataset with 4214 training images and 823 validation images (roughly 16%), which were acquired through Google Open Images V7 [41].

Then the images are fed to a different model for classification. The limited number of images available for training the classification model presented a limitation to the development process. None of the publicly available datasets that were found met the requirements needed for the model's training. In the case of the detection model, the images from Google Open Images V7 were sufficient for prototyping purposes. On the other hand, datasets for object classifications were inadequate, either due to a lack of labeled images for each species or because they included a large number of irrelevant species. To address this issue, a custom dataset was created by compiling labeled images from multiple publicly available datasets on Roboflow Universe [42–48]. These compiled images were also further edited to crop around the fish in the image to replicate the output from the object detector.

As discussed, the cropped images from the frame are fed to the aforementioned object classification model. The primary objective of the image classifier is to first classify the cropped fish images into 5 different species present in Kuwait waters that were gathered for this dataset. The 5 species include Blacktip Sharks, Clownfish, Eagle ray, Emperor Angelfish, and Jellyfish. Approximately 4000 images were gathered for each class, for a total of 24,000 images.

Challenges such as motion blur, low visibility, and dynamic underwater backgrounds are mitigated through data augmentation, ensuring images are augmented with motion blur. Noise was added in order to counter any noise that may come up due to the camera setup. Likewise, the exposure and brightness of the images were augmented in order to deal with the camera's naturally low exposure and the brightness that may be caused due to the flashlights used or darkness present in certain areas. Other techniques such as re-scaling, horizontal flip, and rotation were also used to make the model more robust.

The pipeline makes use of transfer learning with a pre-trained model as part of our project implementation. The pre-trained model chosen for this project is Residual Network 50 (ResNet50) [32]. ResNet50 is a deep learning model, specifically a type of Convolutional Neural Network (CNN), used for tasks such as image classification, object detection, and feature extraction. ResNet50 can be implemented through multiple deep learning libraries. In this case, TensorFlow was used in the implementation. The ImageNet pre-trained weights were used for transfer learning. Furthermore, 50 layers of the ResNet50 model were frozen during training to retain the general features learned on a large dataset. Following this, two dense layers and a dropout layer were also added, and the learning rate was adjusted to 0.000001. The model processes cropped fish images resized to 224×224 pixels, which matches ResNet50's expected input size. The batch size was also adjusted and set to 16. The optimizer of choice for this model was Adam, while the loss function was Categorical Cross-Entropy, as the task involves multi-class classification. Early stopping was also applied to prevent over-fitting.

The pipeline was designed to also be able to detect when an image does not fall into one of the 5 classes ("Unknown" species), enhancing the monitoring application of the pipeline in actual missions. In other words, if the input to the classifier is out-of-distribution, the model is able to identify that and classify the image as such. This is referred to as Anomaly Detection or Novelty Detection. The goal is to flag unusual or suspicious data points that may indicate potential anomalies or abnormalities. Multi-class anomaly detection was chosen and implemented for this project.

Multi-class anomaly detection is an ML technique where the goal is to identify anomalies or outliers across multiple classes or categories simultaneously. In essence, the dataset will be structured normally, but an additional outlier class to represent anomalies will be included. As data were already gathered for the fish detection layer, implementing this method was fairly simple. Aside from the 5 classes for each 5 species discussed previously, an extra class that contains a variety of images of other fish species was gathered and added, raising the total number of images to 40,000.

Once the cropped images are passed to the classifier, and a prediction is given, the output is passed to the pipeline where a second threshold of 80% is applied. If the confidence score of the prediction is above the threshold, one of the six classes (Including "Unknown") will be printed on the frame and displayed along with the bounding box from the object detector. On the other hand, if the confidence score is less than the threshold, "Unknown" will also be printed on the frame. The double-layer confirmation is performed to ensure that the model is robust and that potential anomalies are not overlooked.

5. Results

This section displays the results obtained from testing waterproofing, underwater communication, and the ML model.

5.1. Mechanical Operations

This subsection outlines the testing and validation of key mechanical operations, including the waterproofing of 3D-printed components and wire glands, as well as the

performance evaluation of the ROUV's BLDC and water pump motors in various underwater scenarios.

5.1.1. Waterproofing

Testing was conducted before and after applying the epoxy resin layers. Initially, each 3D printed part was first weighed and then submerged in a water-filled container for 4 h. The 3D-printed parts were then taken out, dried, and weighed again. The results obtained show that the water added a weight that varied between 100 g and 500 g per piece relative to the size of the print, thus proving that waterproofing the parts is essential.

In order to test the wire glands, dummy wires equal to the total number of wires needed at each gland were passed through, and a small amount of instant epoxy was used to fill the openings between the wires. After the epoxy was cured, the WTC was submerged for an hour as well (without the electrical components) and tested for leakage. In this case, no leakage was found.

5.1.2. Motor Functionality

As previously mentioned in Section 4.2.2, Nu utilized two modes of transportation, namely the long-distance mode that uses two BLDC motors and the precision mode with four water pump motors. In this section, both of these modes, along with the sinking and surfacing functionality, were tested in the same body of water mentioned previously. First, Nu was lowered and the peristaltic motors were used to fill the syringes with water. It took approximately 20 s to either fill or empty the syringes. After Nu was submerged, the BLDC motors were operated to drive Nu forward. The BLDC motors allowed Nu to travel at approximately 0.3 m/s, producing a lot of ripples in the process. The water pumps were also tested, and while they were slower in speed, they did not produce any visible ripples on the surface of the water, proving they are well suited for locomotion near marine life.

The ROUV was operational for 4 h continuously on a 2 h charge while all the motors were being used, and it still had charge to spare. A GitHub repository showcasing videos of Nu operating underwater can be found in [49] alongside other materials.

5.2. Communication Systems and Machine Learning

This subsection explores the integration of underwater wireless communication using LoRa technology and the evaluation of an ML-based object detection pipeline, highlighting their effectiveness in enhancing data transmission, fish detection, and classification within real-world aquatic environments.

5.2.1. Underwater Communication

As mentioned in Seciton 1, traditional wireless systems in ROUVs suffer from limitations in range due to the rapid attenuation of high radio frequencies in underwater environments. Technologies such as Wi-Fi or Bluetooth, which utilize higher frequencies, have a range of about 0.1 to 0.5 m underwater [50,51]. This limits what ROUVs can accomplish. As mentioned previously, the low-radio-frequency LoRa module was chosen to address these concerns.

An experiment was conducted to test the validity of the usage of a LoRa module for communication. The LoRa module was placed in an airtight container and then submerged slowly into a body of water while another LoRa module on the surface was continuously sending packets. To make sure that the packets were being delivered successfully, a simple LED system with a relay module was connected to the submerged LoRa module and then monitored for change. The LoRa module maintained its connectivity until the bottom of the body of water was reached at a depth of 2.5 m. This was a result at least five times as good as the alternatives, proving the effectiveness of the LoRa module.

5.2.2. Machine Learning Model Results

The object detector was initially evaluated visually on the validation dataset. Figure 10a,b illustrates a batch of validation images with their ground truth labels alongside the same batch labeled using the model's predictions. As shown in the figures, the model demonstrates high predictive accuracy, often labeling individual fish in the image with greater precision than the provided labels. This discrepancy arises from the nature of the dataset used. As mentioned earlier, the training and validation images for the detection model were sourced from Google Open Images for prototyping purposes. However, this affected the evaluation of the model's performance.

Figure 11 depicts a confusion matrix, which shows a summary of the predictions. The confusion matrix contains four entries: True Positive (TP), True Negative (TN), False Positive (FP), and False Negative (FN). As depicted in Figure 11, the model's ability to detect individual fish, which were labeled as groups in the dataset, results in inaccurate False Positive and False Negative counts. Nevertheless, the model's precise detection significantly simplifies the process of cropping individual fish from the images. The following equations utilize the data in Figure 11 to represent the metrics used to assess the model:

$$Sensitivity(Recall) = R = \frac{TP}{TP + FN} = \frac{1850}{1850 + 1176} = 0.611 = 61.1\% \tag{4}$$

$$Precision = P = \frac{TP}{TP + FP} = \frac{1850}{1850 + 1091} = 0.629 = 62.9\% \tag{5}$$

$$F\text{-}Score = \frac{2PR}{P + R} = \frac{2 \times 0.611 \times 0.629}{0.611 + 0.629} = 0.62 = 62\% \tag{6}$$

$$AccuracyRate = \frac{TP + TN}{TotalSamples} = \frac{1850 + 920}{4} \times 5037 = 0.55 = 55\% \tag{7}$$

As shown in Equations (4)–(7), the model shows adequacy in its key metrics, with an average result of 60% across all key metrics. Recall is the ability of the model to correctly identify all instances of fish present in the dataset. Considering that one of the main aims of the ML model is the detection of "unknown" species, ensuring that the recall value does not fall below a value of 50% is of great importance. A result of 61.1% demonstrates the model's ability to detect fish species effectively, though some instances may still go undetected. The precision reflects that 62.9% of the detected fish species were correctly classified, highlighting moderate reliability in avoiding false positives. However, this result is acceptable, as it is more important to ensure all instances of fish are detected. The F-score, a harmonic mean of precision and recall, stands at 62%, indicating a balanced trade-off between these two metrics. This suggests the model achieves reasonable detection accuracy while minimizing missed or incorrect classifications. Lastly, the accuracy rate shows that the model correctly classified 55% of all instances (true positives and true negatives) in the dataset. Although this indicates room for improvement, the results demonstrate the potential for real-time monitoring and classification of fish species within the operational scope of the Nu submarine. These results show that there is potential for further refinement, such as enhancing dataset quality to ensure that the values for TP, TN, FP, and FN are more accurate or hyperparameter optimization. The enhancement of dataset quality was outside the scope of this paper.
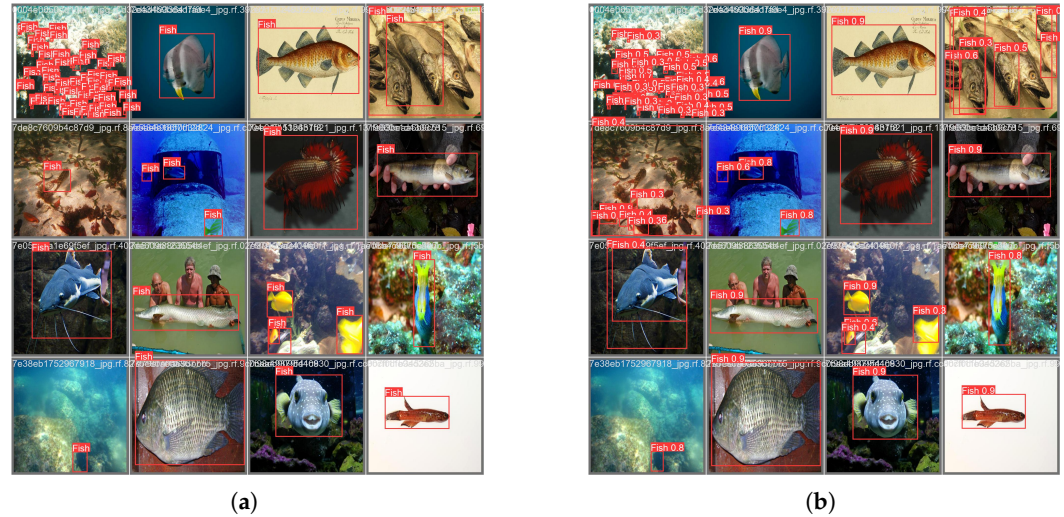
Figure 10. Validation batch: labels and predictions. (**a**) Validation batch labels. (**b**) Validation batch predictions.
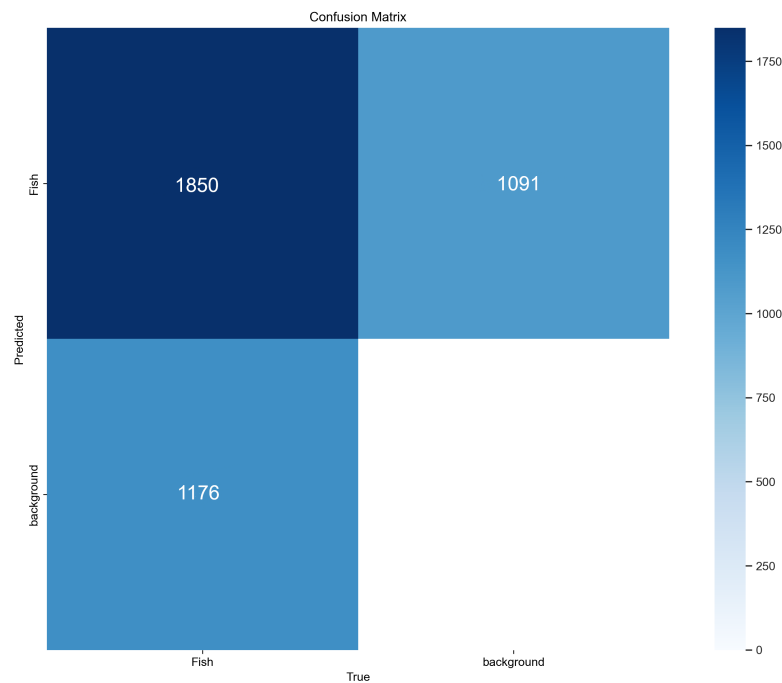

Figure 11. Confusion matrix.

Figure 12a,b showcase the results for the second layer of the pipeline. As can be seen in the accuracy graph, the training curve quickly converges with the validation curve in an upward trend. The accuracy curves climb up to 97% accuracy.

The Loss Graph also shows the training loss converging with the validation loss in a downward trend, noting that the validation loss is lower than its training counterpart, suggesting that the model has a harder time working with the training data. This occurs due to the dropout application during the training.

The convergence of both graphs shows that the model does not suffer from either over-fitting or under-fitting, suggesting that the model is learning successfully from the training data and proving that the model's complexity and generalization in real-life scenarios are sufficient for the task.
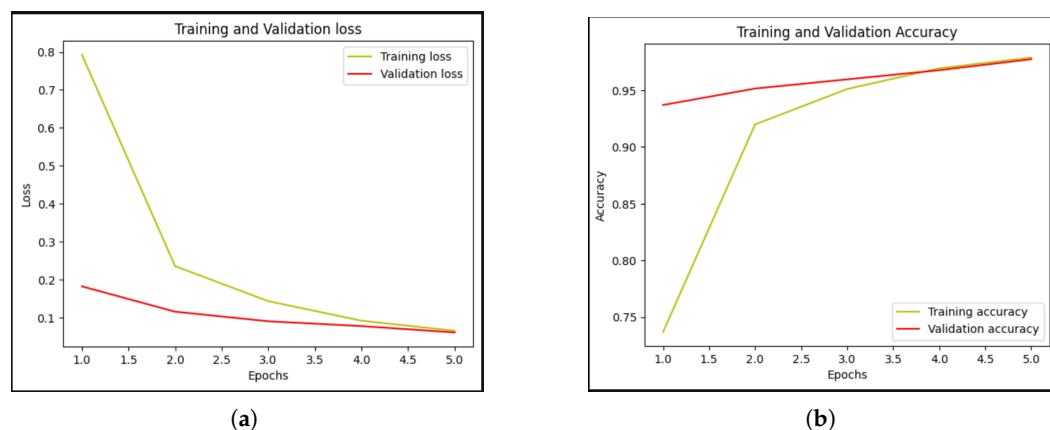
Figure 12. Training and validation loss and accuracy curves. (**a**) Loss learning curve. (**b**) Accuracy learning curve.

Two more stages of testing were conducted after the models were ready for deployment. The first stage involved the usage of images and videos to test the pipeline's capability for detection and classification in a real-life scenario. These videos were fed directly to the model without Nu's involvement. Figure 13a showcases the final pipeline running and detecting fish species in multiple videos. Some of the videos used were shot personally in Kuwaiti waters to test the final pipeline. The videos include both known and unknown fish species.

The second stage of testing, depicted in Figure 13b, involved directly using the onboard camera on Nu for the detection. Various images of different fish species were acquired for this stage. Some of the images were altered by increasing the hue or applying different filters to fully test out the model's full capabilities. Furthermore, Nu's flashlight was also turned on. These steps were taken to better emulate field conditions the proposed system is likely to encounter. Finally, the images were laminated, and the model was tested in a pool. The model's performance was better than what the theoretical calculations indicated. It managed to accurately detect all the laminated images, only showing some inaccuracies when the images were approximately 4 to 5 m from the camera. Furthermore, despite the blur applied to some of the images and the flashlight's interference, the pipeline correctly classified each species and managed to classify anomalous data points accurately.
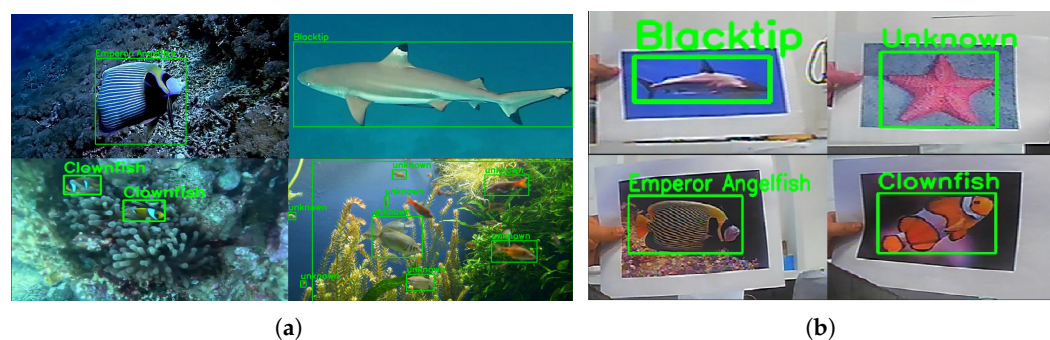

Figure 13. Pipeline classification testing: (**a**) High-quality images. (**b**) Low-quality images (tested using the onboard camera).

6. Conclusions

This paper introduced Nu, a wireless ROUV system that is capable of identifying and classifying fish species through a live camera feed in real-time. While operational, the ROUV minimized damage to the species and their habitat with the implementation

of two modes of transportation: long-distance mode and precision mode. The long-distance mode utilized BLDC motors that provided high speeds, while the precision mode minimized disturbance to marine life and utilized water pump motors that suck water from one end and push it out the other. The ROUV employed LoRa as its main communication technology with the operator, which proved to be a reliable option due to its long range, low power consumption, and low frequency, where higher frequencies tend to attenuate easily underwater. Using the onboard camera with its own battery and communication systems, a live-feed video is received on a laptop and displayed to the operator. Through an ML pipeline, the live-feed video is analyzed and the results are displayed in real time. The first layer of the pipeline detected all the fish in the feed. Once they are detected, a bounding box is drawn, and each fish is then cropped and passed to the second layer. The second layer classified the fish into one of five species in the database: Blacktip Sharks, Clownfish, Eagle ray, Emperor Angelfish, and Jellyfish, all of which are available in Kuwait's seas. If the model fails to classify the image into one of the five classes, a sixth Unknown class is used. With the mentioned functionalities, Nu cuts down costs on exploration expeditions while simultaneously reducing the damage done to underwater species and habitats, as well as reducing the health risks imposed on divers while diving deep underwater for prolonged periods of time. Future directions include developing an additional ROUV within the system to transport the identification ROUV to its designated expedition area, thereby conserving power and enabling the deployment of a coordinated swarm of identification ROUVs to collect and integrate fish classification data efficiently.

Abbreviations

The following abbreviations are used in this manuscript:

ROUV	Remotely Operated Underwater Vehicle
ROV	Remotely Operated Vehicle
AUV	Autonomous Underwater Vehicle

LoRa	Long Range
WTC	Water Tight Chamber
ML	Machine Learning
AI	Artificial Intelligence
PVC	Polyvinyl Chloride
GUI	Graphical User Interface
NIR	Near-Infrared
GCS	Ground Control Station
BLDC	Brushless Direct Current
PLA	Poly-lactic Acid
FDM	Fused Deposition Modeling
ESC	Electronic Speed Controller
CNN	Convolutional Neural Network

References

1. Vermeij, G.J.; Grosberg, R.K. The Great Divergence: When Did Diversity on Land Exceed That in the Sea? *Integr. Comp. Biol.* **2010**, *50*, 675–682. [CrossRef] [PubMed]
2. How Much of the Ocean Have We Explored? Available online: https://oceanservice.noaa.gov/facts/exploration.html (accessed on 1 October 2024).
3. Why Do We Explore the Ocean? Available online: https://oceanexplorer.noaa.gov/facts/why.html#:~:text=Information (accessed on 1 October 2024).
4. Aeroshark. Available online: https://www.lufthansa-technik.com/en/aeroshark (accessed on 1 October 2024).
5. Feng, J.C.; Liang, J.; Cai, Y.; Zhang, S.; Xue, J.; Yang, Z. Deep-sea organisms research oriented by deep-sea technologies development. *Sci. Bull.* **2022**, *67*, 1802–1816. [CrossRef] [PubMed]
6. Terrón-Sigler, A.; León-Muez, D.; Peñalver-Duque, P.; Torre, F.E. The effects of SCUBA diving on the endemic Mediterranean coral Astroides calycularis. *Ocean Coast. Manag.* **2016**, *122*, 1–8. [CrossRef]
7. Apps, K.; Heagney, E.; Thi Khanh Ngoc, Q.; Dimmock, K.; Benkendorff, K. Scuba divers, coral reefs, and knowledge of ocean acidification. *Mar. Policy* **2023**, *155*, 105779. [CrossRef]
8. Todnem, K.; Nyland, H.; Skeidsvoll, H.; Svihus, R.; Rinck, P.; Kambestad, B.K.; Riise, T.; Aarli, J.A. Neurological long term consequences of deep diving. *Occup. Environ. Med.* **1991**, *48*, 258–266. [CrossRef]
9. Bellingham, J. Platforms: Autonomous Underwater Vehicles. In *Encyclopedia of Ocean Sciences*, 3rd ed.; Cochran, J.K., Bokuniewicz, H.J., Yager, P.L., Eds.; Academic Press: Oxford, UK, 2009; pp. 159–169. [CrossRef]
10. Stenius, I.; Folkesson, J.; Bhat, S.; Sprague, C.I.; Ling, L.; Özkahraman, O.; Bore, N.; Cong, Z.; Severholt, J.; Ljung, C.; et al. A System for Autonomous Seaweed Farm Inspection with an Underwater Robot. *Sensors* **2022**, *22*, 5064. [CrossRef]
11. Bell, K.; Chow, J.; Hope, A.; Quinzin, M.; Cantner, K.; Amon, D.; Cramp, J.; Rotjan, R.; Kamalu, L.; De Vos, A.; et al. Low-Cost, Deep-Sea Imaging and Analysis Tools for Deep-Sea Exploration: A Collaborative Design Study. *Front. Mar. Sci.* **2022**, *9*, 873700. [CrossRef]
12. Zhang, S.; Wei, S.; Liu, Z.; Li, T.; Li, C.; Huang, X.; Wang, C.; Xie, Z.; Al-Hartomy, O.; Al-Ghamdi, A.; et al. The rise of AI optoelectronic sensors: From nanomaterial synthesis, device design to practical application. *Mater. Today Phys.* **2022**, *27*, 100812. [CrossRef]
13. Augustin, A.; Yi, J.; Clausen, T.; Townsley, W.M. A Study of LoRa: Long Range & Low Power Networks for the Internet of Things. *Sensors* **2016**, *16*, 1466. [CrossRef]
14. Devalal, S.; Karthikeyan, A. LoRa technology—An overview. In Proceedings of the 2018 Second International Conference on Electronics, Communication and Aerospace Technology (ICECA), Coimbatore,India, 29–31 March 2018; IEEE: New York, NY, USA, 2018; pp. 284–290.
15. Bor, M.C.; Vidler, J.; Roedig, U. LoRa for the Internet of Things. In Proceedings of the Ewsn, Graz, Austria, 15–17 February 2016; Volume 16, pp. 361–366.
16. Peppas, K.; Chronopoulos, S.K.; Loukatos, D.; Arvanitis, K. New Results for the Error Rate Performance of LoRa Systems over Fading Channels. *Sensors* **2022**, *22*, 3350. [CrossRef]
17. Ubidots. LoRaWAN vs NB-IoT: A Comparison Between IoT Trend-Setters. *Ubidots Blog* **2024**. Available online: https://ubidots.com/blog/lorawan-vs-nb-iot/ (accessed on 23 October 2024).
18. Al-Hindi, K.; Al-Muallem, M.; Al-Adwani, G.; Faqiha, K.; Bantan, R.; Zamzami, A.; Abdel Gawad, A. *Radio-Controlled-Submarine Model for Engineering Education*; The Military Technical College: Cairo, Egypt, 2017.

19. Dang, T.; Lapierre, L.; Zapata, R.; Ropars, B.; Gourmelen, G. A Dynamically Reconfigurable Autonomous Underwater Robot for Karst Exploration: Design and Experiment. *Sensors* **2022**, *22*, 3379. [CrossRef] [PubMed]
20. Salem, K.M.; Rady, M.; Aly, H.; Elshimy, H. Design and Implementation of a Six-Degrees-of-Freedom Underwater Remotely Operated Vehicle. *Appl. Sci.* **2023**, *13*, 6870. [CrossRef]
21. Aguirre-Castro, O.A.; Inzunza-González, E.; García-Guerrero, E.E.; Tlelo-Cuautle, E.; López-Bonilla, O.R.; Olguín-Tiznado, J.E.; Cárdenas-Valdez, J.R. Design and Construction of an ROV for Underwater Exploration. *Sensors* **2019**, *19*, 5387. [CrossRef] [PubMed]
22. Carreras, M.; Candela, C.; Ribas, D. Sparus II, design of a lightweight hovering AUV. In Proceedings of the 5th International Workshop on Marine Technology (MARTECH), Girona, Spain, 9–11 October 2013; pp. 163–164.
23. Pae, B.; Chen, D. Miniature submarine using near-infrared spectroscopy to detect and collect microplastics. *Int. J. High Sch. Res.* **2022**, *4*, 88–93. [CrossRef]
24. Abenanth, G.K.; Balachander, s.; Sivakarthikeyan, U.; Avinash Subramaniam, M.; Aravinth, J. Design and Construction of a Submarine Miniature. In Proceedings of the 2020 International Conference on Communication and Signal Processing (ICCSP), Melmaruvathur, India, 28–30 July 2020; pp. 0061–0066. [CrossRef]
25. Cowan, M.; Phillips, C.; Sklivanitis, G. Towards Wireless Controlled Underwater Vehicles. In Proceedings of the Global Oceans 2020: Singapore–U.S. Gulf Coast, Biloxi, MS, USA, 5–30 October 2020; pp. 1–5. [CrossRef]
26. Delina, M.; Taryudi.; Amin, M.F.; Hussaan, A.M.; Trismidianto.; Arifin, F.I.; Syah, S.M.I. The Development of Remotely Operated Underwater Vehicle for Plastic Waste Detection with Raspberry Pi. *J. Phys. Conf. Ser.* **2024**, *2866*, 012048. [CrossRef]
27. Kim, B.C.; Kim, H.C.; Han, S.; Park, D.K. Inspection of Underwater Hull Surface Condition Using the Soft Voting Ensemble of the Transfer-Learned Models. *Sensors* **2022**, *22*, 4392. [CrossRef]
28. Gong, B.; Dai, K.; Shao, J.; Jing, L.; Chen, Y. Fish-TViT: A novel fish species classification method in multi water areas based on transfer learning and vision transformer. *Heliyon* **2023**, *9*, e16761. [CrossRef]
29. Jalal, A.; Salman, A.; Mian, A.; Shortis, M.; Shafait, F. Fish detection and species classification in underwater environments using deep learning with temporal information. *Ecol. Informatics* **2020**, *57*, 101088. [CrossRef]
30. White, F.M. *Fluid Mechanics*, 8th ed.; McGraw-Hill Education: New York, NY, USA, 2016.
31. Varghese, R.; Sambath, M. YOLOv8: A Novel Object Detection Algorithm with Enhanced Performance and Robustness. In Proceedings of the 2024 International Conference on Advances in Data Engineering and Intelligent Computing Systems (ADICS), Chennai, India, 18–19 April 2024; pp. 1–6. [CrossRef]
32. He, K.; Zhang, X.; Ren, S.; Sun, J. Deep Residual Learning for Image Recognition. *arXiv* **2015**, arXiv:1512.03385.
33. Chapman, A. How to 3D Print Waterproof Parts. Available online: https://ultimaker.com/learn/how-to-3d-print-waterproof-parts/#:~:text=A (accessed on 29 October 2024).
34. Fu, Y.; Michopoulos, J.G.; Song, J. On Investigating the Thermomechanical Properties of Cross-linked Epoxy Via Molecular Dynamics Analysis. *J. Appl. Polym. Sci.* **2019**, *136*, 47633. [CrossRef]
35. University of Cambridge. Properties of FDM Prints. Available online: https://www.doitpoms.ac.uk/tlplib/add_manuf/fdm.php (accessed on 29 October 2024).
36. Ryecroft, S.; Shaw, A.; Fergus, P.; Kot, P.; Hashim, D.; Moody, A.; Conroy, L. A First Implementation of Underwater Communications in Raw Water Using the 433 MHz Frequency Combined with a Bowtie Antenna. *Sensors* **2019**, *19*, 1813. [CrossRef]
37. Smart Projects. *Arduino UNO R3 Microcontroller*. 2010. Available online: https://docs.arduino.cc/resources/datasheets/A000066-datasheet.pdf (accessed on 11 November 2024).
38. Semtech Corporation. *LoRa SX1278 433Mhz Module*. 2013. Available online: https://cdn-shop.adafruit.com/product-files/3179/sx1276_77_78_79.pdf (accessed on 11 November 2024).
39. *KY-023 Joystick Module*. Available online: https://naylampmechatronics.com/img/cms/Datasheets/000036%20-%20datasheet%20KY-023-Joy-IT.pdf (accessed on 11 November 2024).
40. Jiangsu JQC Electronics. *JQC-3FF-S-Z Module*. Available online: https://www.generationrobots.com/media/JQC-3FF-v1.pdf (accessed on 11 November 2024).
41. Krasin, I.; Duerig, T.; Alldrin, N.; Ferrari, V.; Abu-El-Haija, S.; Kuznetsova, A.; Rom, H.; Uijlings, J.; Popov, S.; Kamali, S.; et al. Open Images Dataset V7. A Large-Scale Dataset for Object Detection, Image Classification, and Visual Relationship Detection. 2020. Available online: https://storage.googleapis.com/openimages/web/index.html (accessed on 15 March 2024).
42. Blacktipreefsharkdetection. Blacktip_Reef_Shark_Detection Dataset. 2024. Available online: https://universe.roboflow.com/blacktipreefsharkdetection/blacktip_reef_shark_detection (accessed on 29 November 2024).
43. BD. WhiteBlackTipShark Dataset. 2023. Available online: https://universe.roboflow.com/bd-l2nym/whiteblacktipshark (accessed on 29 November 2024).
44. Detection, F. Emperor Angelfish Dataset. 2024. Available online: https://universe.roboflow.com/fish-detection-fmwtf/emperor-angelfish-jy8yr (accessed on 29 November 2024).

45. camarine1. TRaining2 Dataset. 2021. Available online: https://universe.roboflow.com/camarine1/training2-rjbp0 (accessed on 29 November 2024).

46. Clownfish. Clownfish Dataset. 2024. Available online: https://universe.roboflow.com/clownfish/clownfish-1dyxx (accessed on 29 November 2024).

47. Fishes, S.N. EagleRay New Dataset. 2023. Available online: https://universe.roboflow.com/seami-new-5-fishes/eagleray-new (accessed on 29 November 2024).

48. Hust. jellyfish_data Dataset. 2022. Available online: https://universe.roboflow.com/hust-mze6f/jellyfish_data (accessed on 30 November 2024).

49. Dafar, T. Available online: https://github.com/Dafar01/NU-ROUV (accessed on 15 November 2024).

50. Taniguchi, Y. Experimental Evaluation of a WiFi Device in an Undersea Environment. In Proceedings of the 2015 3rd International Conference on Artificial Intelligence, Modelling and Simulation (AIMS), Kota Kinabalu, Malaysia, 2–4 December 2015; pp. 408–411. [CrossRef]

51. Harun-Or-Rashid, M.; Biswas, D. Design and Fabrication of an Unmanned Underwater Vehicle. In Proceedings of the International Conference on Mechanical, Industrial and Energy Engineering, Khulna, Bangladesh, 23–24 December 2018.